ELSEVIER

Toxicon 45 (2005) 929–939

TOXICON

www.elsevier.com/locate/toxicon

Structural analysis of the catalytic domain of tetanus neurotoxin

Krishnamurthy N. Rao[a], Desigan Kumaran[a], Thomas Binz[b], Subramanyam Swaminathan[a,*]

[a]*Brookhaven National Laboratory, Biology Department, 50 Bell Avenue, Upton, NY 11973, USA*
[b]*Department of Biochemistry, Medizinischule Hochschule Hannover, Hannover, Germany*

Received 10 December 2004; revised 16 February 2005; accepted 17 February 2005
Available online 13 April 2005

Abstract

Clostridium neurotoxins, comprising the tetanus neurotoxin and the seven antigenically distinct botulinum neurotoxins (BoNT/A-G), are among the known most potent bacterial protein toxins to humans. Although they have similar function, sequences and three-dimensional structures, the substrate specificity and the selectivity of peptide bond cleavage are different and unique. Tetanus and botulinum type B neurotoxins enzymatically cleave the same substrate, vesicle-associated membrane protein, at the same peptide bond though the optimum length of substrate peptide required for cleavage by them is different. Here, we present the first experimentally determined three-dimensional structure of the catalytic domain of tetanus neurotoxin and analyze its active site. The structure provides insight into the active site of tetanus toxin's proteolytic activity and the importance of the nucleophilic water and the role of the zinc ion. The probable reason for different modes of binding of vesicle-associated membrane protein to botulinum neurotoxin type B and the tetanus toxin is discussed. The structure provides a basis for designing a novel recombinant vaccine or structure-based drugs for tetanus.
Published by Elsevier Ltd.

Keywords: *Clostridium* neurotoxin; Tetanus neurotoxin; Botulinum neurotoxin; Zinc; Metalloprotease; Dual-wavelength anomalous diffraction (DAD); X-ray structure

1. Introduction

Tetanus neurotoxin (TeNT) produced by *Clostridium tetani* and the seven antigenically distinct botulinum neurotoxins (BoNT/A-G) produced by *Clostridium botulinum* together constitute the family of clostridial neurotoxins (CNTs) (Montecucco and Schiavo, 1995; Rawlings and Barrett, 1995). Tetanus neurotoxin acts on the central nervous system and inhibits the release of glycine and γ-aminobutyric acid causing spastic paralysis, tetanus (Galazka and Gasse, 1995). In contrast, botulinum neurotoxins (BoNTs) act on the peripheral nervous system and inhibit the release of acetylcholine at the neuromuscular junction, causing flaccid paralysis, botulism (Simpson, 1986). These proteins are of public health concern as paralysis by these toxins still takes hundreds of lives every year (Galazka and Gasse, 1995). They are also emerging as biowarfare threats.

CNTs consist of three functional domains: binding, translocation, and catalytic. CNTs bind to the neuronal cells via gangliosides and a second protein receptor and then are internalized. Their catalytic domain is translocated through the vesicle membrane into the cytosol where it attacks and cleaves one of the proteins forming the core of the synaptic vesicle fusion apparatus. CNTs synthesized as 150 kDa inactive single chain molecules are post-translationally modified either by endogenous or exogenous proteases into two polypeptide chains covalently linked by a disulfide bond: the C-terminal heavy chain (HC, 100 kDa)

* Corresponding author. Tel.: +1 631 344 3187; fax: +1 631 344 3407.
E-mail address: swami@bnl.gov (S. Swaminathan).

0041-0101/$ - see front matter Published by Elsevier Ltd.
doi:10.1016/j.toxicon.2005.02.032

and the N-terminal light chain (LC, 50 kDa). The C-terminal heavy chain is responsible for the binding of the toxin to specific neuronal receptors and the translocation of the N-terminal LC, the catalytic domain, into the neuronal cytosol. The LCs of CNTs contain the zinc-binding motif HExxH + E and are accordingly zinc-dependent metalloproteinases causing toxicity (Eswaramoorthy et al., 2004; Fillippis et al., 1995; Kurazono et al., 1992; Schiavo et al., 1994; Simpson et al., 2001). Interestingly, though CNTs display high sequence homology, have similar functions and probably have similar structure, they are unique in that their target protein and the scissile bonds they cleave are different, a property very commonly shared by members of a given protease family. TeNT, BoNT/B, /D, /F, and /G cleave vesicle-associated membrane protein (VAMP) (Schiavo et al., 2000). While the cleavage site is different for D, F and G, it is the same for TeNT and BoNT/B, a unique case in CNTs. Similarly, BoNT/A, /E, and C cleave synaptosomal-associated protein 25 kDa (SNAP-25) at different peptide bonds (Binz et al., 1994; Schiavo et al., 1993; Vaidyanathan et al., 1999). BoNT/C is unique in that it also cleaves syntaxin.

Chemically modified TeNT is the most used human vaccine and BoNTs are increasingly used in the therapy of human diseases caused by hyperfunction of cholinergic nerve terminals (Jankovic and Hallett, 1994). Chemically treated toxoid vaccine is available against BoNTs but no therapeutic treatments exist as of now. To develop an effective structure-based vaccine/inhibitor/antitoxin to treat tetanus victims, an understanding of the molecular mechanism at the atomic level, especially the peptidase activity by the catalytic domain, is a prerequisite. Though experimental three-dimensional structures are available for some of the CNTs and their functional fragments, no experimental structure is available for TeNT-LC except for a homology-based model (Agarwal et al., 2004a; Breidenbach and Brunger, 2004; Emsley et al., 2000; Hanson and Stevens, 2000; Lacy and Stevens, 1998; Rossetto et al., 2001; Segelke et al., 2004; Swaminathan and Eswaramoorthy, 2000; Umland et al., 1997). These structures helped to map the active site and the residues forming it. Although the active sites are similar, the specificity and selectivity of CNTs suggest that there must be additional factors that define the substrate specificity. Thus, it becomes important to understand the molecular structure of each of the CNTs at the atomic level to gain insight into their unique ability to cleave at specific scissile bonds within the same substrate and also among different substrates. A possible catalytic mechanism has been proposed for TeNT from the homology model (Rossetto et al., 2001). Extensive mutational studies have been carried out on TeNT (Li et al., 1994; McMahon et al., 1993; Yamasaki et al., 1994). Some of these mutants were proteolytically inactive indicating that they may have a direct role in the catalytic activity of the protease. However, there was no matching X-ray structural information available to interpret these results. The chemical characterization of the active site and of the residues involved in zinc binding of TeNT is important to understand the mechanism of the proteolytic activity of this novel family of metalloproteases (Montecucco and Schiavo, 1995; Schiavo et al., 1994) and may lead to the development of novel and safer recombinant vaccine produced outside of *C. tetani*. A crystal structure analysis provides a tremendous amount of insight into both the structure and the function of the protein. Although the crystallization of TeNT-LC has been reported, no experimental structure is available in literature (Tonello et al., 1994). Here, we present the first experimental three-dimensional structure of TeNT-LC and compare it with the crystal structures of available BoNT-LC structures.

2. Materials and methods

2.1. Expression and purification of his-tagged TeNT-LC protein

The procedure for expression and purification is as described in Agarwal et al. (2004b) except that ampicillin-containing medium was used. The protein was eluted from Ni-NTA agarose columns with increasing concentrations of imidazole buffer. Fractions of the eluate were analyzed by SDS-PAGE using 4–20% gels followed by staining with Coomassie blue. A ~52 kDa band corresponding to TeNT-LC reproducibly eluted in 50–100 mM imidazole fractions was obtained. Recovery of TeNT-LC was more than 4 mg/l of induced cell culture. At this stage, it is nearly 80% pure. TeNT-LC was further purified by gel filtration on a (2×20 in.) column of Superdex-75 using Akta FPLC which also helped in exchanging the buffer from phosphate to 20 mM HEPES, pH 7.2 + 200 mM NaCl. Peak fractions containing only pure TeNT-LC were pooled and concentrated to ~10.0 mg/ml using Centriprep YM-10.

2.2. Enzymatic activity of TeNT-LC

The proteolytic activity of TeNT-LC was assayed in vitro on its substrate VAMP which had an N-terminal GST tag. The assay was performed in a final volume of 20 μL [20 mM HEPES, pH 7.4, 2 mM DTT, 10 μM $Zn(CH_3COO)_2$] containing a 10–5000 nM concentration of LC and a 5 μM concentration of VAMP and the mixtures were incubated at 37 °C for 30 min. The reactions were stopped by adding 10 μl of 3× concentrated SDS-PAGE sample buffer. The extent of cleavage was then evaluated following SDS-PAGE (4–20% gels) by the appearance and intensity of a new band at ~30 kDa due to the cleavage of GST–VAMP at Gln76–Phe77 peptide bond of VAMP. A 1000 nM concentration of LC was required to cleave 50% of the substrate in 30 min.

2.3. Crystallization

The crystallization screening was carried out by the sitting drop vapor diffusion method using Hampton Research high throughput crystallization screens and TECAN Genesis Freedom crystallization robot. One microlitre of the protein solution containing 10 mg/ml protein, 200 mM NaCl, and 20 mM HEPES buffer at pH 7.2 was combined with 1 μl of the precipitant and equilibrated against 600 μl of the same precipitant. Diffraction-quality crystals obtained at room temperature using 20% PEG 4000, 0.2 M $MgCl_2$, and 0.1 M HEPES at pH 7.0 as precipitant grew to their full size in about 4 weeks. Mother liquor containing 15–20% glycerol proved to be a good cryoprotectant for collecting X-ray diffraction data at liquid nitrogen temperature. Crystal data are presented in Table 1.

2.4. Data collection

Data were collected at liquid nitrogen temperature at the National Synchrotron Light Source, Brookhaven National Laboratory. Since the protein contains one zinc ion per molecule, dual-wavelength anomalous dispersion (DAD) data were collected from a wild-type LC crystal at wavelengths 1.2810 and 1.2824 Å, corresponding to the peak and inflection of the zinc absorption edge at beamline X12C, NSLS with a CCD-based Brandeis B4 detector. Data covering a total of 360° rotation in ϕ were collected for an oscillation range of 1° per frame. However, the diffraction limit extended to 3.0 Å only. Higher resolution data to 2.4 Å resolution were later collected at beamline X25, NSLS. Data were processed with HKL2000 (Otwinowski and Minor, 1997). Details of data collection statistics are given in Table 1.

2.5. Structure determination

The peak and edge data were used to locate the position of zinc atom using SOLVE (Terwilliger and Berendzen, 1997). Initial model phases were also calculated by the molecular replacement method using AmoRe with BoNT/B-LC (PDB idcode: 1F82) as search model (Navaza and Saludjian, 1997). AmoRe gave a good starting model with *R* and correlation coefficient of 0.47 and 0.58, respectively. Phases obtained with zinc were refined by SHARP (De-La-Fortelle and Bricogne, 1997) using the model phases as external phases and further improved by density modification (Cowtan, 1994). The molecular model with the sequence of TeNT-LC was built using the program O (Jones et al., 1991). At this stage, since higher resolution data were available, they were used in the refinement.

Table 1
Data collection and refinement statistics

	Crystal-I		Crystal-II
Space group	*C222*		*C222*
Cell parameters	$a=105.49$ Å, $b=176.92$ Å, and $c=57.45$ Å		$a=106.61$ Å, $b=177.29$ Å, and $c=54.55$ Å
Phasing			
Method: DAD	Peak	Edge	Native
Wavelength (Å)	1.2810	1.2824	1.10
Anomalous scatterer	Zinc	Zinc	
Resolution (Å)	50–3.0	50–3.0	50–2.4
No. of reflections	15,350	15,365	20,639
Rmerge[a] (%)	0.13 (0.35)	0.13 (0.35)	0.12 (0.39)
Overall completeness (%)	99.8 (99.3)	98.5 (98.1)	99.4 (99.1)
Redundancy	13.3 (9.7)	12.8 (9.3)	9.4 (9.3)
Overall FOM	0.20		
After solvent flattening	0.90		
Refinement statistics			
Resolution range (Å)	50–2.6		
No. of reflections	15,170		
Overall completeness (%)	92.7 (90)		
R-factor	0.21		
R-free	0.27		
No. of protein atoms	3221		
No. of heterogen atoms	1		
No. of water molecules	113		
RMS deviations			
Bond lengths (Å)	0.007		
Bond angles (°)	1.33		

[a] The values corresponding to the outermost shell are given within parentheses. Rmerge is as defined in HKL2000. FOM, R-factor and R-free are as defined in SHARP program.

After initial rigid body refinement, the structure was further refined using CNS (Brunger et al., 1998). Solvent molecules were added from the difference Fourier map. The protein model is complete except for residues 64–67, 208–219, 252–264 which are in the loop regions and for about 30 C-terminal residues, for which the electron density is poorly defined, indicating these regions may be disordered. The final *R* and *R*-free values are 0.21 and 0.27, respectively. The structure has been validated with PROCHECK (Laskowski et al., 1993), and the distribution of residues in the Ramachandran plot is given in Table 1. Coordinates have been deposited with the Protein Data Bank (1YVG).

3. Results

3.1. Structure of TeNT-LC

TeNT-LC forms a dimer in the crystal via a crystallographic two-fold with about 10% (3100 Å^2) of the total surface area buried at the interface. A Ribbons representation of the catalytic domain dimer of TeNT-LC along with the active site residues is shown in Fig. 1a. All of the LC structures so far determined, except BoNT/B-LC, exist as dimer either via crystallographic or non-crystallographic two-fold. While the dimeric interface covers the active site

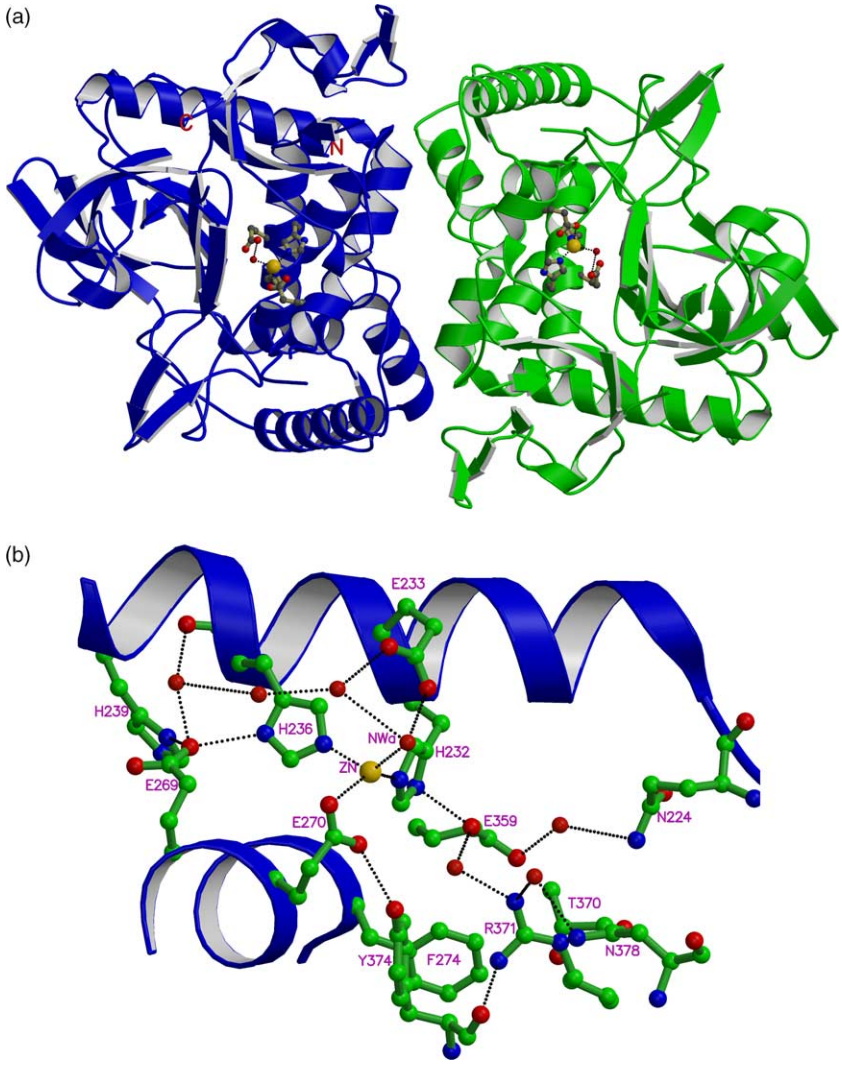

Fig. 1. (a) Ribbons representation of a dimer of TeNT-LC, with zinc and the coordinating residues shown in the ball-and-stick model. The dimer is formed by a crystallographic two-fold symmetry passing through the mid point normal to the plane of the figure. (b) The active site of TeNT-LC showing the interactions and hydrogen bonding network involving the residues that are nearly conserved in TeNT, BoNT/B, /E and /A LCs. Hydrogen bonds are shown as dashed lines in black. The nucleophilic water molecule coordinated with zinc is labeled 'NWa'.

zinc in BoNT/A-LC, the active sites are exposed to the solvent region in BoNT/E and TeNT-LCs.

As in other LC structures, the active site of TeNT-LC is located deep inside a cavity by which the substrate gains access to the active site. The active site is centered around a zinc cation coordinated by a strictly conserved HExxH + E motif. In TeNT-LC, zinc is directly coordinated by residues His232, His236 and Glu270 (the numbering scheme is as in Swiss-Prot: P04958) (Fig. 1b). The fourth ligand is a nucleophilic water molecule that also forms a strong hydrogen bond with Glu233. The coordinating distances are given in Table 2. The coordination geometry at zinc is slightly distorted from tetrahedral geometry. The δ-carboxyl group of Glu233 serves to coordinate the hydrogen-bonded nucleophilic water molecule in one of the four tetrahedral positions around the catalytic zinc ion. This interaction seems to be important for the activation of the nucleophilic water. In most zinc endopeptidases, the substrate or an inhibitor displaces the nucleophilic water and moves it closer to the glutamate residue serving as proton shuttling agent. Because of this movement, the nucleophilic water would make stronger hydrogen bonds (possibly two) with the proton shuttling glutamate, making it a strong nucleophile (Swaminathan et al., 2004). The residues coordinated with the zinc form a primary sphere of residues centered around the active site and their direct role in catalysis has been confirmed through site-directed mutagenesis studies (Li et al., 1994; Rossetto et al., 2001; Yamasaki et al., 1994). From mutagenesis experiments, it also appears that residues in the secondary layer near the active site are essential or play a crucial role in the catalytic function. These residues found in the vicinity (within 10 Å from zinc) of the active site zinc include Glu233, His239, Phe274, Glu359, Thr370, Arg371, Tyr374, and Asn378. Among these, mutation of Glu233, His239, Phe274, Arg371 and Tyr374 residues in TeNT and the corresponding residues in BoNTs resulted in complete or partial loss of the catalytic activity indicating their direct role in catalytic function. These residues are found farther than 3.0 Å from the zinc or the nucleophilic water and their interacting distances are given in Table 2. These along with a few water molecules form hydrogen bonds to the residues coordinated with the zinc ion (Fig. 1b), indicating that these residues are essential for the stability of the structure and/or the conformation of the active site.

Table 2
Active site residues interacting distances (Å) in TeNT, BoNT/B, and /E LC structures

	TeNT-LC (Å)	BoNT/ B-LC (Å)	BoNT/ E-LC (Å)
Zn–H232 NE2	2.37	2.11	2.18
Zn–H236 NE2	2.13	2.15	2.16
Zn–E270 OE1	2.49	2.60	2.22
Zn–E270 OE2	2.46	2.20	2.46
Zn–Nu. water	2.50	2.08	2.17
Nu. water–E233OE1	3.84	3.54	4.03
Nu. water–E233OE2	3.09	2.80	2.82
Nu. water–Y374–OH	6.06	4.62	3.56
Nu. water–E270 OE1	3.62	3.11	3.15
Nu. water–R371NH2	7.90	7.46	7.06
E359OE1–H232ND1	2.65	2.71	2.61
E359OE2–R371NH1	4.42	3.04	2.99
E269OE1–H236ND1	2.79	3.03	2.76
E269OE1–H239ND1	2.58	2.73	2.73
Y374–OH–Zn	5.37	4.30	3.94
Y374–OH–E270OE1	3.10	3.69	3.15
Y374–OH–E270OE2	4.48	3.70	3.43
R371NH–Zn	7.29	6.50	7.08

The numbering scheme corresponds to TeNT.

The TeNT-LC model excludes the 60 (residues 64–67), 200 (residues 208–219) and 250 (residues 252–264) loops since the electron density is poorly defined in these regions. Residues in these loop regions, in general, appear disordered in all LC structures. A probable reason is that they lose hydrophobic interactions with the translocation domain that were present in the holotoxin on separation or lack of it in the recombinant LC. The C-terminal region which forms the central strand of a β sheet with the two outer strands from the translocation domain in the holotoxin may similarly be disordered. These catalytic domain loops were observed to change their conformation significantly upon separation from the holotoxin and subsequent binding of the substrate in the case of BoNT/B (Hanson and Stevens, 2000). In fact, the substrate is found to bind between these loops. Thus, efficient proteolysis of the substrate seems dependent on the movement of these loops because it exposes the binding surface of the catalytic domain and brings the catalytic residues in position and facilitates the catalysis. Unfortunately, the poorly defined electron density prevents a detailed comparison of these loops with those of substrate bound and unbound BoNT/B-LC. However, when the model of TeNT-LC is superposed on native or substrate bound BoNT/B-LC, the weak electron density at least allows tracing the direction of these loops. Thus, it is very likely that these loops in TeNT-LC undergo similar rearrangement upon substrate binding as in the case of BoNT/B-LC and, in addition, this cooperative change is supported based on kinetic data on TeNT (Cornille et al., 1997). Comparison with BoNT/B-LC and the packing consideration of the *C222* space group suggest that the orientation of these loops may be different from BoNT/B-LC as otherwise there will be steric interactions. The position of loop 140 (residues 140–148) in TeNT-LC looks to be different than that observed in BoNT/B-LC. The loop 140 of TeNT-LC is tilted away from the corresponding BoNT/B-LC loop with the farthest distance between corresponding residues being approximately 12 Å. A possibility that the missing residues in the 250 loop may be due to auto catalysis as in the case of BoNT/A-LC was ruled out since the SDS-PAGE gel analysis showed no such indication (Segelke et al., 2004). The disorder in the C-terminal region seems to be common

to all LCs. This may also be due to the lack of the interchain disulfide bond.

3.2. Comparison with other CNT LCs

The structure of TeNT-LC is similar to those of BoNT/A, B, and E-LCs indicating that all the LCs of CNTs have similar structure and are unique only in that they have stringent substrate specificity. The specificity of CNTs is therefore likely to arise from the residues that form the channel by which the substrate gains access to the active site and the complementarity of substrate and the enzyme residues. When the C_α atoms of TeNT-LC were superimposed onto those of BoNT-LCs using the program LSQMAN the rms deviation varied between 1 and 1.4 Å (1.02 Å for 380 C_α of BoNT/B, 1.2 Å for 350 C_α of BoNT/E, 1.4 Å for 340 C_α of BoNT/A) (Kleywegt and Jones, 1997). A stereo view of the C_α trace of TeNT-LC superimposed on other BoNT-LC models is shown in Fig. 2a. The TeNT-LC structure superimposes better with BoNT/B than with BoNT/A or BoNT/E-LC. This is not surprising since TeNT and BoNT/B have the substrate specificity and scissile bond selectivity for VAMP among these CNTs. This may also be partly because TeNT and BoNT/B LCs share 52% sequence identity which is greater than that (∼35%) shared by all clostridial neurotoxin LCs (Kurazono et al., 1992; Lacy and Stevens, 1999). An alignment of sequences of LCs of TeNT, and BoNT/B is shown in Fig. 3.

When the active sites of TeNT and BoNT/B are superposed, they preserve some of the structural features involving a few conserved residues. These include Asn168, Glutamate residues 169, 233, 269, 359, His239, Thr273, Arg371, Ile235 and Phe274 and the zinc-binding motif residues HExxH (Fig. 2b). Many of the interactions established by these residues are common to all CNTs (Agarwal et al., 2004a). However, it is intriguing to note here that although TeNT and BoNT/ B process the same peptide bond in VAMP, there are some differences in details near the active site. Three catalytically important residues,

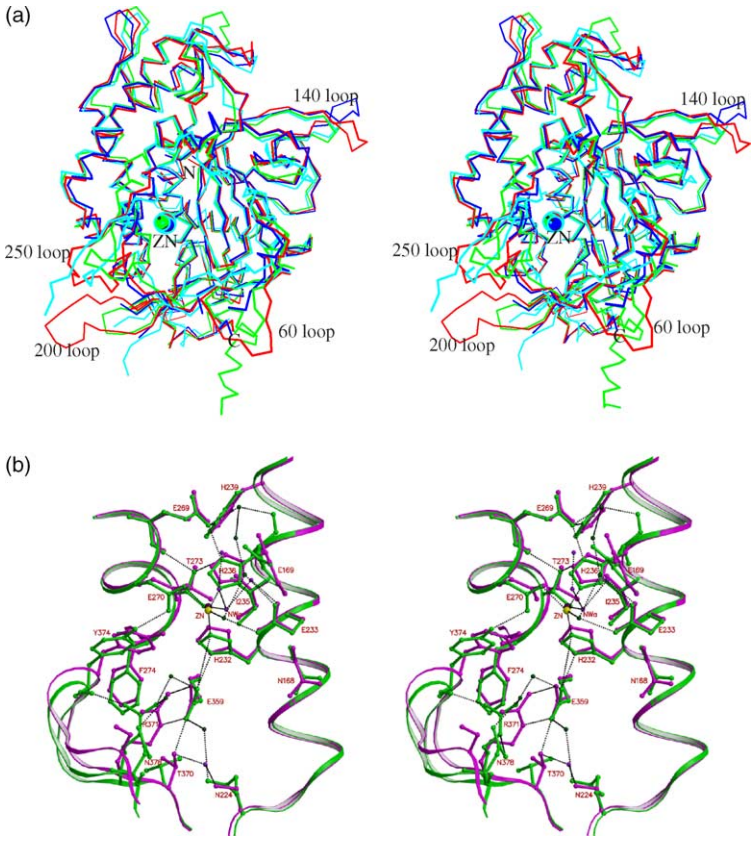

Fig. 2. (a) Stereo view of a superposition of C_α traces of TeNT (blue), BoNT/B (red), /E (green), /A (light blue). The conformations of all the LCs are similar except for the loop regions. The loops 60, 200 and 250 are incomplete in the TeNT-LC structure. The loop140 points in the opposite directions in TeNT and BoNT/B LCs. Zinc atoms are shown in different sizes for clarity. (b) Stereo view of a superposition of the active sites of TeNT (green) and BoNT/B (magenta) LCs showing the differences in the interactions of the three catalytically important residues Glu359, Arg371 and Tyr374 in the two LC structures. The residues shown are within 10 Å distance from the zinc position. The interactions involving the hydrogen bonds are shown in dashed lines. The water molecules of TeNT are shown in dark green and those of BoNT/B are shown in purple.

```
TENT            PITINNFRYSDPVNNDTIIMMEPPYCKGLDIYYKAFKITDRIWIVPERYEFGTKPEDFNP 60
BONT/B          PVTINNFNYNDPIDNNNIIMMEPPFARGTGRYYKAFKITDRIWIIPERYTFGYKPEDFNK 60
                *:*****.*.**::*:.*******:.:* . **************:**** ** ******

TENT            PSSLIEG-ASEYYDPNYLRTDSDKDRFLQTMVKLFNRIKNNVAGEALLDKIINAIPYLGN 119
BONT/B          SSGIFNRDVCEYYDPDYLNTNDKKNIFLQTMIKLFNRIKSKPLGEKLLEMIINGIPYLGD 120
                .*.:::  ..*****:**.*:..*: *****:*******.:  ** **: ***.*****:

TENT            SYSLLDKFDTNSNSVSFNLLEQDPSGATTKSAMLTNLIIFGPGPVLNKNEVRGIVLRVDN 179
BONT/B          RRVPLEEFNTNIASVTVNKLISNPGEVERKKGIFANLIIFGPGPVLNENET----IDIGI 176
                    *::*:**  **:.* * .:*. .  *..:::************:**.    : :.

TENT            KNYFPCRDGFGSIMQMAFCPEYVPTFDNVIENITSLTIGKSKYFQDPALLLMHELIHVLH 239
BONT/B          QNHFASREGFGGIMQMKFCPEYVSVFNNVQENKGASIFNRRGYFSDPALILMHELIHVLH 236
                :*:*..*:***.**** ******..*:** **  :  :.:  **.****:**********

TENT            GLYGMQVSSHEIIPSKQEIYMQHTYPISAEELFTFGGQDANLISIDIKNDLYEKTLNDYK 299
BONT/B          GLYGIKVDDLPIVPNEKKFFMQSTDAIQAEELYTFGGQDPSIITPSTDKSIYDKVLQNFR 296
                ****::*..  *:*.:::::** * .*.****:******..:*: . .:.:*:*.*:::: 

TENT            AIANKLSQVTSCN-DPNIDIDSYKQIYQQKYQFDKDSNGQYIVNEDKFQILYNSIMYGFT 358
BONT/B          GIVDRLNKVLVCISDPNININIYKNKFKDKYKFVEDSEGKYSIDVESFDKLYKSLMFGFT 356
                .*.::*.:*  *  ****:*: **: :::**:* :**:*:* :: :.*: **:*:*:*** 

TENT            EIELGKKFNIKTRLSYFSMNHDPVKIPNLLDDTIYNDTEGFNIESKDLKSEYKGQNMRVN 418
BONT/B          ETNIAENYKIKTRASYFSDSLPPVKIKNLLDNEIYTIEEGFNISDKDMEKEYRGQNKAIN 416
                * ::.::::**** **** .  **** **** **.  *****..**::.**:***  :* 

TENT            TNAFRNVDGSGLVSKLIGLCKKIIPPTNIRENLYNRT 455
BONT/B          KQAYEEISKEHLAVYKIQMCKSVKAPG---------- 443
                .:*:.::. . *.   * :**.: .*
```

Fig. 3. The alignment of sequences of TeNT and BoNT/B LCs using CLUSTAL-W. The residues seen within 4 Å distance from the substrate VAMP are highlighted. The residues coordinated to zinc are in bold inside the box. The bottom line represents the degree of homology—'*' identical, ':' conserved and '.' semiconserved.

Glu359, Arg371 and Tyr374, were found to be different with respect to their position and interactions they make near the active site (Fig. 2b). Through mutagenesis experiments on TeNT and BoNT/A-LCs and structural studies on various serotypes of BoNTs, it has been shown that these residues are involved in the catalysis (Agarwal et al., 2004a; Binz et al., 2002; Hanson and Stevens, 2000; Rossetto et al., 2001; Segelke et al., 2004). In TeNT, the OE1 atom of Glu359 forms a hydrogen bonded interaction with ND1 atom of the His232, which is coordinated with the zinc ion, and thus helps in orienting the side chain of His232. The Glu359 side chain OE1 and OE2 atoms are held in position through hydrogen bond interactions with two water molecules. These two water molecules in turn interact with NH2 of Arg371 and NE2 of Asn224. However, in BoNT/B the side chain atoms of the equivalent Glu357 directly interact with the NH2 of the equivalent Arg369 and OG1 of Thr368. The side chain of the equivalent residue Thr370 in TeNT-LC is positioned away from this site. However, the side chain of Asn224 in TeNT-LC provides an interaction. Interestingly, the position of Asn224 in TeNT-LC is occupied by Ser221 in BoNT/B-LC (Fig. 2b).

The NE, NH1 and NH2 atoms of Arg371 in TeNT interact with OD1 of Asn378, the main chain O atom of Tyr374 and a water molecule, respectively. However, NE and NH2 atoms of the equivalent Arg369 in BoNT/B interact with OE2 and OE1 atoms of Glu357, whereas the NH1 atom of Arg369 is too far away to interact with the main chain O atom of Tyr372. As a result, in BoNT/B-LC the Arg369 is close to Glu357 but is away from the Tyr372. In contrast, in TeNT the equivalent Arg371 moves away from the Glu359 but is close to Tyr374 and one more aromatic residue Phe274. Recently, mutation of the equivalent Phe266 in BoNT/A-LC was shown to have an effect on the catalytic activity of the toxin (Rigoni et al., 2001). The side chain of Arg371 in TeNT is positioned in between the aromatic planes of the Tyr374 and Phe274, so that the guanidino group of Arg371 interacts with the π electron clouds of the two aromatic rings to neutralize their charge (Fig. 2b). These amino–aromatic electrostatic interactions were observed to occur in the range of 3.6–6 Å (max at 4.7 Å) distance in proteins (Burley and Petsko, 1986). The NH1 atom of Arg371 was found to be at a distance of 4.18 and 3.95 Å from the aromatic planes of Tyr374 and Phe274, respectively. However, in BoNT/B-LC, these electrostatic interactions seem to be stabilized through interaction between Arg369 and Glu357.

The OH-group of Tyr374 in TeNT forms a hydrogen bond with Glu270 OE1, which in turn is coordinated with

the zinc ion (Fig. 2b). This interaction seems to be important to hold the side chain of the residue Glu270 in position. The corresponding residue in BoNT/B (Tyr372) has been implicated to be involved in stabilizing the cleaved product of the substrate by donating a proton to the leaving group, Phe77, of the VAMP (Hanson and Stevens, 2000). This hydrogen bond mediated interaction is absent in BoNT/B-LC. However, the side chain of the residue Tyr372 in BoNT/B is at a distance of 4.3 Å from the catalytic zinc ion, but the equivalent distance in TeNT is 5.37 Å. It is not clear whether this has an effect on the catalytic activity.

3.3. Differential mode of VAMP binding to TeNT and BoNT/B-LCs

Both TeNT and BoNT/B cleave VAMP at the same peptide bond, Gln76–Phe77. Nevertheless, appreciable divergence in their sequence (52% similar) reflects some differences between the two enzymes. Indeed, the two enzymes were observed to be different in their proteolytic activities towards different minimum sized VAMP substrates, pH and temperature profiles, and sensitivity to inhibitors such as captopril. It was suggested that these differences could be a consequence of subtle differences in their intracellular actions and due to fine structural details at the atomic level (Foran et al., 1994). It has been shown that BoNT/B cleaves a peptide corresponding to the VAMP segment encompassing residues 55–94 while TeNT requires residues 33–94, an amino-terminal extension of 22 residues, to cleave efficiently (Cornille et al., 1997; Foran et al., 1994; Pellizzari et al., 1996). The minimum length of substrate peptide for BoNT/B contains only the second (V2) of the two SNARE Secondary Recognition (SSR) motifs; but for TeNT the optimum substrate length contains both SSR motifs of VAMP, V1 and V2 (38–47 and 62–71). In general, it is the residues spanning the cleavage site in a substrate, which define the efficiency of a protease. Since these toxins require different minimal substrate length, they must recognize their substrate in a unique but different fashion. Studies based on mutation of VAMP residues, and antibodies raised against motif peptides or recombinant proteins have suggested that TeNT and BoNT/B were similar in their recognition of SSR motifs (Pellizzari et al., 1996). With the currently determined three-dimensional structure of TeNT-LC, it is clear that the LCs of TeNT and BoNT/B fold very similarly and their active site architecture exhibits extensive similarity although with some differences in H-bonding interactions. Hence, the difference in minimum length peptide required for activity cannot be explained by the sole recognition of the cleavage site. This might suggest that the binding interactions required for positioning the substrate for cleavage may be different. Taking together these observations, it is very likely that TeNT and BoNT/B bind VAMP at the same site but their mode of binding may differ. Thus the two toxins are likely to have extended substrate-binding regions in which a large number of amino acids interact with moieties away from the active site. Indeed, in the crystal structure of BoNT/B bound substrate product, the substrate and the protease have numerous interactions remote from the active site (Hanson and Stevens, 2000).

An extensive analysis in terms of three-dimensional structure to pinpoint the differences that may be responsible for unique recognition of VAMP by TeNT and BoNT/B LCs was carried out. First, the TeNT-LC structure was superposed on BoNT/B-LC to be in the same orientation. Then the VAMP peptide was positioned similar to its orientation in BoNT/B-LC (Hanson and Stevens, 2000). The amino acid residues that are interacting within 4 Å distance from VAMP residues that are conserved in space were compared (Fig. 4). About 50 residues that fall within 4 Å from the substrate are highlighted in Fig. 3. This excluded the residues that are within coordinating distance from the zinc ion, because they process the identical scissile bond. These residues did not differ with respect to their C_α positions in the two toxins as their position remains the same when compared to the unbound BoNT/B structure. The comparison revealed that only 30% of these residues are conserved. Forty percent of the residues differed between TeNT and BoNT/B LCs with respect to their hydrophilic or hydrophobic nature. About 30% of the residues in TeNT had bulkier side chains when compared to the residues in BoNT/B. The 30% conserved residues may have common interactions with the substrate in both the toxins. Thus, these conserved residues can be thought of as the minimal essential residues to recognize the substrate by the two toxins. The 40% residues that provide different environment with respect to their hydrophobic or hydrophilic nature around the substrate may be responsible for the differential mode of substrate binding by TeNT and BoNT/B. The 30% residues of TeNT that are bulkier (shown in yellow, Fig. 4a) compared to those in BoNT/B make steric clashes with the VAMP residues, if it were to bind as in BoNT/B. These residues would destabilize the binding of substrate by the protease. The observation that the TeNT requires extra 22 N-terminal residues for optimal activity compared to BoNT/B can be explained as follows. TeNT-LC needs to interact with a more extended segment of the substrate compared to BoNT/B-LC to stabilize the enzyme–substrate complex. The affinity to the substrate segment shared with BoNT/B could be lower. This fact is evident from comparison of the TeNT-LC structure with that of the BoNT/B structure bound to VAMP. Out of the 40 residues of VAMP bound to BoNT/B, 13 would make steric clashes in TeNT. Of this 13, five residues (Glu62, Asp64, Asp65, Asp68, and Gln71) of the substrate are in the V2 region. For example, Met377 of TeNT would produce a very short contact with Asp 68 of VAMP. This might not allow the V2 region to come close to the enzyme for binding in contrast to BoNT/B. This could be compensated by the binding of V1 to the enzyme. There are two possibilities. The V2 region and the adjacent N terminal region of the substrate could project out like a hair pin

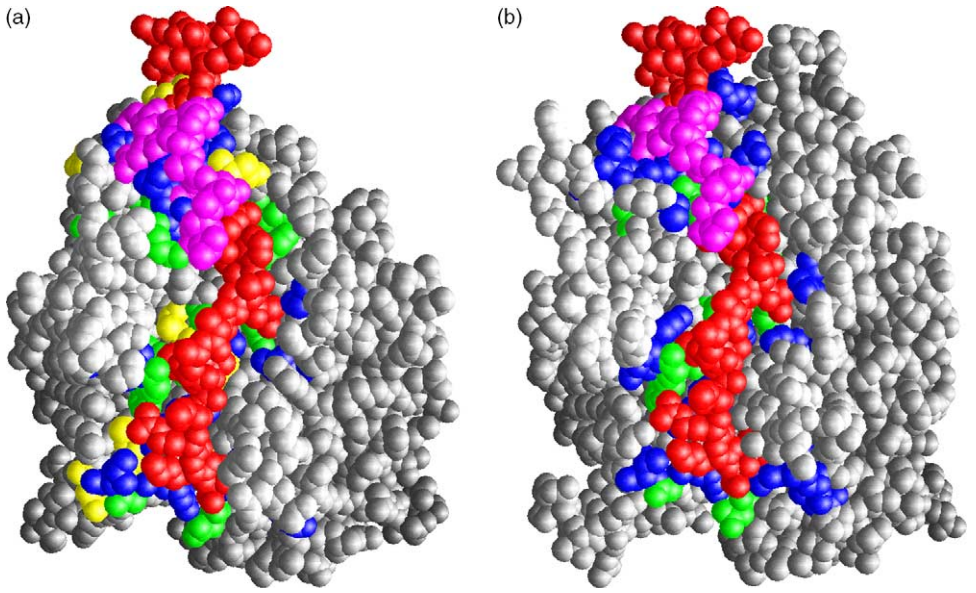

Fig. 4. (a) Sphere model representation of TeNT-LC with the substrate VAMP peptide placed in a similar position and orientation as in the BoNT/B–VAMP complex crystal structure (Hanson and Stevens, 2000). (b) Sphere model representation of BoNT/B bound to peptide VAMP. VAMP residues are shown in red except the V2 region, which is in magenta. Residues in TeNT-LC and BoNT/B-LC within 4 Å of the VAMP peptide are shown in green for conserved residues and blue if they are different. Residues which are bulkier in TeNT compared to BoNT/B are shown in yellow. The apparent difference in the shapes of TeNT-LC and BoNT/B-LC is due to the absence of some loops in TeNT-LC.

allowing the V1 region to bind in the same place as V2 in BoNT/B or the steric clash would push V2 away from the surface and V1 could bind to the enzyme in a shallow region on the other side of the molecule to increase the binding constant. However, since Asp64 and Asp68 of V2 are conserved in V1, and Asp65 of V2 is replaced by Glu41 in V1, we prefer the second possibility. These collective observations suggest that TeNT and BoNT/B interact differently with VAMP and provide a base for the design of effective inhibitors for both toxins. This situation could be similar to what was shown for BoNT/A or /E where the absence of one of the SSR motif is compensated by one of the other three SSRs (Washbourne et al., 1997).

4. Conclusion

Tetanus and botulinum neurotoxins are solely responsible for the neuroparalytic syndromes of tetanus and botulism. Considering the importance of tetanus neurotoxin in human pathology and therapeutics, there is an immediate demand for three-dimensional structural information, especially of the catalytic domain. The present experimental structure fulfils this need. Currently, anti-tetanus vaccine is prepared by chemical modification of toxin with formaldehyde. However, it is believed that genetically modified toxins better preserve immunogenicity than chemical modification and such a vaccine based on a mutated bacterial toxin is already in use as anti-pertussis vaccine (Rappuoli et al., 1992). The present crystal structure study provides a basis for developing a novel anti-tetanus vaccine through rational design of genetically modified protein and also in designing structure-based small molecule inhibitors.

Acknowledgements

Research supported by the US Army Medical Research Acquisition Activity (Award No. DAMD17-02-2-0011) under DOE Prime Contract No. DE-AC02-98CH10886 with Brookhaven National Laboratory. T.B. was supported by a grant RGY0027/2001 from Human Frontier Science Program. We would like to thank Drs A. Saxena and M. Becker for providing beamtime at the NSLS and Drs R. Agarwal, S. Eswaramoorthy and S. Jayaraman for helpful discussions.

References

Agarwal, R., Eswaramoorthy, S., Kumaran, D., Binz, T., Swaminathan, S., 2004a. Structural analysis of botulinum neurotoxin type E catalytic domain and its mutant Glu212→Gln reveals the pivotal role of the Glu212 carboxylate in the catalytic pathway. Biochemistry 43, 6637–6644.

Agarwal, R., Eswaramoorthy, S., Kumaran, D., Dunn, J.J., Swaminathan, S., 2004b. Cloning, high level expression,

purification and crystallization of the full length *Clostridium botulinum* neurotoxin type E light chain. Protein Expr. Purif. 34, 95–102.

Binz, T., Blasi, J., Yamasaki, S., Baumeister, A., Link, E., Sudhof, T.C., Jahn, R., Niemann, H., 1994. Proteolysis of SNAP-25 by Types E and A botulinum neurotoxins. J. Biol. Chem. 269, 1617–1620.

Binz, T., Bade, S., Rummel, A., Kollewe, A., Alves, J., 2002. Arg^{362} and Tyr^{365} of the botulinum neurotoxin type A light chain are involved in transition state stabilization. Biochemistry 41, 1717–1723.

Breidenbach, M.A., Brunger, A., 2004. Substrate recognition strategy for botulinum neurotoxin serotype A. Nature 432, 925–929.

Brunger, A.T., Adams, P.D., Clore, G.M., Delano, W.L., Gros, P., Grosse-Kunstleve, R.W., Jiang, J.S., Kuszwewski, J., Nilges, M., Pannu, N.S., Read, R.J., Rice, L.M., Somonsom, T., Warren, G.L., 1998. Crystallography and NMR system: a new software suite for macromolecular structure determination. Acta Crystallogr. D54, 905–921.

Burley, S.K., Petsko, G.A., 1986. Amino–aromatic interactions in proteins. FEBS Lett. 203, 139–143.

Cornille, F., Martin, L., Lenoir, C., Cussac, D., Roques, B.P., Fourine-Zaluski, M., 1997. Cooperative exosite dependent cleavage of synapotbrevin by tetanus toxin light chain. J. Biol. Chem. 272, 3459–3464.

Cowtan, K., 1994. Joint CCP4 ESF-EACBM Newslett. Protein Crystallogr. 31, 34–38.

De La Fortelle, E., Bricogne, G., 1997. Maximum-likelihood heavy atom parameter refinement in the MIR and MAD methods. Meth. Enzymol. 276, 472–493.

Emsley, P., Fotinou, C., Black, I., Fairweather, N.F., Charles, I.G., Watts, C., Hewitt, E., Isaacs, N.W., 2000. The structures of the H(C) fragment of tetanus toxin with carbohydrate subunit complexes provide insight into ganglioside binding. J. Biol. Chem. 275, 8889–8894.

Eswaramoorthy, S., Kumaran, D., Keller, J., Swaminathan, S., 2004. Role of metals in the biological activity of *Clostridium botulinum* neurotoxins. Biochemistry 43, 2209–2216.

Fillippis, V.D., Vangelista, L., Schiavo, G., Tonello, F., Montecucco, C., 1995. Structural studies on the zinc-endopeptidase light chain of tetanus neurotoxin. Eur. J. Biochem. 229, 61–69.

Foran, P., Shone, C.C., Dolly, J.O., 1994. Differences in the protease activities of tetanus and botulinum B toxins revealed by the cleavage of vesicle-associated membrane protein and various sized fragments. Biochemistry 33, 15365–15374.

Galazka, A., Gasse, F., 1995. The present status of tetanus and tetanus vaccination. Curr. Top. Microbiol. Immunol. 195, 31–53.

Hanson, M.A., Stevens, R.C., 2000. Cocrystal structure of synaptobrevin-ll bound to botulinum neurotoxin type B at 2.0 A resolution. Nat. Struct. Biol. 7, 687–692.

Jankovic, J., Hallett, M., 1994. Therapy with Botulinum Toxin. Marcel Dekker, New York.

Jones, T.A., Zou, J., Cowtan, S., Kjeldgaard, M., 1991. Improved methods in building protein models in electron density map and the location of errors in these models. Acta Crystallogr. A47, 110–119.

Kleywegt, G.J., Jones, T.A., 1997. Detecting folding motifs and similarities in protein structures. Meth. Enzymol. 277, 525–545.

Kurazono, H., Mochida, S., Binz, T., Eisel, U., Quanz, M., Grebenstein, O., Wernars, K., Poulain, B., Tauc, L., Niemann, H., 1992. Minimal essential domains specifying toxicity of the light chains of tetanus toxin and botulinum neurotoxin type A. J. Biol. Chem. 267, 14721–14729.

Lacy, D.B., Stevens, R.C., 1998. Unravelling the structures and modes of action of bacterial toxins. Curr. Opin. Struct. Biol. 8, 778–784.

Lacy, D.B., Stevens, R.C., 1999. Sequence homology and structural analysis of clostridial neurotoxins. J. Mol. Biol. 291, 1091–1104.

Laskowski, R.A., MacArthur, M.W., Moss, D.S., Thornton, J.M., 1993. PROCHECK: a program to check the stereochemical quality for assessing the accuracy of protein structures. J. Appl. Crystallogr. 26, 283–291.

Li, Y., Foran, P., Fairweather, N.F., de Paiva, A., Weller, U., Dougan, G., Dolly, J.O., 1994. A single mutation in the recombinant light chain of tetanus toxin abolishes its proteolytic activity and removes the toxicity seen after reconstitution with native heavy chain. Biochemistry 33, 7014–7020.

McMahon, H.T., Ushkaryov, Y.A., Edelmann, L., Link, E., Binz, T., Niemann, H., Jahn, R., Sudhof, T.C., 1993. Cellubrevin is a ubiquitous tetanus-toxin substrate homologous to a putative synaptic vesicle fusion protein. Nature 364, 346–349.

Montecucco, C., Schiavo, G., 1995. Structure and function of tetanus and botulinum neurotoxins. Q. Rev. Biophys. 28, 423–472.

Navaza, J., Saludjian, P., 1997. AMoRe: an automated molecular replacement program package. Meth. Enzymol. 276, 581–594.

Otwinowski, Z., Minor, W., 1997. Processing of X-ray diffraction data collected in oscillation mode. Meth. Enzymol. 276, 307–326.

Pellizzari, R., Rossetto, O., Lozzi, L., Giovedi', S., Johnson, E., Shone, C.C., Montecucco, C., 1996. Structural determinants of the specificity for synaptic vesicle-associated membrane protein/synaptobrevin of tetanus and botulinum type B and G neurotoxins. J. Biol. Chem. 271, 20353–20358.

Rappuoli, R., Podda, A., Pizza, M., Covacci, A., Bartoloni, A., de Magistris, M.T., Nencioni, L., 1992. Progress towards the development of new vaccines against whooping cough. Vaccine 10, 1027–1032.

Rawlings, N.D., Barrett, A.J., 1995. Evolutionaly families of metallopeptidases. Meth. Enzymol. 248, 183–228.

Rigoni, M., Caccin, P., Johnson, E.A., Montecucco, C., Rossetto, O., 2001. Site-directed mutagenesis identifies active-site residues of the light chain of botulinum neurotoxin type A. Biochem. Biophys. Res. Commun. 288, 1231–1237.

Rossetto, O., Caccin, P., Rigoni, M., Tonello, F., Bortoletto, N., Stevens, R.C., Montecucco, C., 2001. Active-site mutagenesis of tetanus neurotoxin implicates TYR-375 and GLU-271 in metalloproteolytic activity. Toxicon 39, 1151–1159.

Schiavo, G., Santucci, A., Dasgupta, B.R., Metha, P.P., Jontes, J., Benfenati, F., Wilson, M.C., Montecucco, C., 1993. Botulinum neurotoxins serotypes A and E cleave SNAP-25 at distinct COOH-terminal peptide bonds. FEBS Lett. 335, 99–103.

Schiavo, G., Rossetto, O., Benfenati, F., Poulain, B., Montecucco, C., 1994. Tetanus and botulinum neurotoxins are zinc proteases specific for components of the neuroexocytosis apparatus. Ann. NY. Acad. Sci. 710, 65–75.

Schiavo, G., Matteoli, M., Montecucco, C., 2000. Neurotoxins affecting neuroexocytosis. Physiol. Rev. 80, 717–766.

Segelke, B., Knapp, M., Kadkhodayan, S., Balhorn, R., Rupp, B., 2004. Crystal structure of *Clostridium botulinum* neurotoxin protease in a product-bound state: evidence for noncanonical zinc protease activity. Proc. Natl Acad. Sci. USA 101, 6888–6893.

Simpson, L.L., 1986. Molecular pharmacology of botulinum toxin and tetanus toxin. Annu. Rev. Pharmacol. Toxicol. 26, 427–453.

Simpson, L.L., Maksymowych, A.B., Hao, S., 2001. The role of zinc binding in the biological activity of botulinum toxin. J. Biol. Chem. 276, 27034–27041.

Swaminathan, S., Eswaramoorthy, S., 2000. Structural analysis of the catalytic and binding sites of *Clostridium botulinum* neurotoxin B. Nat. Struct. Biol. 7, 693–699.

Swaminathan, S., Eswaramoorthy, S., Kumaran, D., 2004. Structure and enzymatic activity of botulinum neurotoxins. Mov. Disord. 19 (Suppl. 8), S17–S22.

Terwilliger, T.C., Berendzen, J., 1997. Automated structure solution for MIR and MAD. Acta Crystallogr. D55, 849–861.

Tonello, F., Pellizzari, R., Pasqualato, S., Grandi, G., Peggion, E., Montecucco, C., 1994. Recombinant and truncated tetanus neurotoxin light chain: cloning, expression, purification, and proteolytic activity. Protein Expr. Purif. 15, 221–227.

Umland, T.C., Wingert, L.M., Swaminathan, S., Furey, W.F., Schmidt, J.J., Sax, M., 1997. Structure of the receptor binding fragment H_c of tetanus neurotoxin. Nat. Struct. Biol. 4, 788–792.

Vaidyanathan, V.V., Yoshino, K., Jahnz, M., Dorries, C., Bade, S., Nauenburg, S., Niemann, H., Binz, T., 1999. Proteolysis of SNAP-25 isoforms by botulinum neurotoxin types A, C, and E: domains and amino acid residues controlling the formation of enzyme–substrate complexes and cleavage. J. Neurochem. 72, 327–337.

Washbourne, P., Pellizzari, R., Baldini, G., Wilson, M.C., Montecucco, C., 1997. Botulinum neurotoxin A and E require the SNARE motif in SNAP-25 for proteolysis. FEBS Lett. 418, 1–5.

Yamasaki, S., Hu, Y., Binz, T., Kalkuhl, A., Kurazono, H., Tamura, T., Jahn, R., Kandel, E., Niemann, H., 1994. Synaptobrevin/vesicle-associated membrane protein (VAMP) of *Aplysia californica*: structure and proteolysis by tetanus toxin and botulinal neurotoxins type D and F. Proc. Natl Acad. Sci. USA 91, 4688–4692.